The ISME Journal (2017), 1–12

www.nature.com/ismej

ORIGINAL ARTICLE

Temperature is a key factor in *Micromonas*–virus interactions

David Demory[1,2], Laure Arsenieff[3], Nathalie Simon[3], Christophe Six[3], Fabienne Rigaut-Jalabert[4], Dominique Marie[3], Pei Ge[3], Estelle Bigeard[3], Stéphan Jacquet[5], Antoine Sciandra[1], Olivier Bernard[2], Sophie Rabouille[1] and Anne-Claire Baudoux[3]

[1]*Sorbonne Universités, UPMC Univ Paris 06, CNRS, Villefranche/mer, France;* [2]*BIOCORE-INRIA, BP93, Sophia-Antipolis Cedex, France;* [3]*Sorbonne Universités, UPMC Univ Pierre et Marie Curie (Paris 06), CNRS, Adaptation et Diversité en Milieu Marin UMR7144, Station Biologique de Roscoff, Roscoff, France;* [4]*Sorbonne Universités, UPMC Univ Pierre et Marie Curie (Paris 06), CNRS, Fédération de Recherche FR2424, Station Biologique de Roscoff, Roscoff, France and* [5]*INRA, UMR CARRTEL, Thonon-les-Bains Cedex, France*

The genus *Micromonas* comprises phytoplankton that show among the widest latitudinal distributions on Earth, and members of this genus are recurrently infected by prasinoviruses in contrasted thermal ecosystems. In this study, we assessed how temperature influences the interplay between the main genetic clades of this prominent microalga and their viruses. The growth of three *Micromonas* strains (Mic-A, Mic-B, Mic-C) and the stability of their respective lytic viruses (MicV-A, MicV-B, MicV-C) were measured over a thermal range of 4–32.5 °C. Similar growth temperature optima (T_{opt}) were predicted for all three hosts but Mic-B exhibited a broader thermal tolerance than Mic-A and Mic-C, suggesting distinct thermoacclimation strategies. Similarly, the MicV-C virus displayed a remarkable thermal stability compared with MicV-A and MicV-B. Despite these divergences, infection dynamics showed that temperatures below T_{opt} lengthened lytic cycle kinetics and reduced viral yield and, notably, that infection at temperatures above T_{opt} did not usually result in cell lysis. Two mechanisms operated depending on the temperature and the biological system. Hosts either prevented the production of viral progeny or maintained their ability to produce virions with no apparent cell lysis, pointing to a possible switch in the viral life strategy. Hence, temperature changes critically affect the outcome of *Micromonas* infection and have implications for ocean biogeochemistry and evolution.

The ISME Journal advance online publication, 13 January 2017; doi:10.1038/ismej.2016.160

Introduction

Viruses represent the most abundant biological entities known on Earth and they are likely to infect any form of life in the ocean (Suttle, 2005, 2007). Over the past decades, it has become evident that viruses play a pivotal role in marine ecosystems, especially through their profound influence on the structure and the functioning of microbial communities (see Brum and Sullivan, 2015 for a recent review). The ecological impact of viral infection is however largely determined by the different viral life strategies. Lytic viruses replicate and kill their host by cell lysis. This mode of infection influences ocean productivity and biogeochemistry by altering the dynamics, structure and the function of microbial assemblages (Fuhrman, 1999; Suttle, 2005) but also the recycling of organic matter through the viral shunt (Fuhrman, 1999; Wilhelm and Suttle, 1999; Brussaard *et al.*, 2008). Lysogenic viruses affect the microbial evolution by inserting their own nucleic sequence into their host genome, which may provide the host with new functional traits and immunity against superinfection (Jiang and Paul, 1996; Wilson and Mann, 1997). The ecological incidence of chronic infections, by which viruses disseminate by budding or diffusion through host membranes, has been much less documented in marine ecosystems (Thomas *et al.,* 2011, 2012). Despite the global impact of viral infection in the ocean, the regulation of infection dynamics and the relative share among the different infection strategies remain far from understood (Knowles *et al.,* 2016).

Several field studies have evidenced latitudinal variations of virus-induced mortality in marine microbial assemblages. For example, increasing viral lysis rates of phytoplankton were recorded from high to low latitudes across the North Atlantic Ocean and, interestingly, correlated positively with temperature

Correspondence: D Demory, Laboratoire d'océanographie de Villefranche, UMR 7093, Observatoire Océanographique de Villefranche-sur-Mer, 181 chemin du Lazaret, Villefranche-sur-Mer 06230, France.
E-mail: david.demory@obs-vlfr.fr
Received 30 May 2016; revised 30 September 2016; accepted 7 October 2016

and salinity (Mojica *et al.,* 2015). Consistent with this finding, high incidence of lysogeny and low viral lysis rates were shown to occur in low temperature ecosystems such as polar, mesopelagic and deep-sea waters or during cold periods in temperate systems (McDaniel *et al.,* 2002; Williamson *et al*., 2002; Weinbauer *et al*., 2003; McDaniel *et al*., 2006; Evans *et al*., 2009). These studies suggest that viral life strategies other than lytic infection might prevail in cold environments or periods of low productivity. However, other field studies reported contradictory trends (Cochran and Paul, 1998; Weinbauer and Suttle, 1999) and it is still unclear whether temperature-driven shifts in viral infection dynamics and strategy represent a global pattern or arise from local processes.

Laboratory studies on virus–host model systems in controlled conditions have proven essential to address such fundamental question. These approaches have shown that temperature may influence the infection process by regulating viral abundance and infectivity. Most marine virus isolates tolerate low temperatures whereas increasing temperatures tend to induce loss in infectivity and ultimately inactivation of the viral particles (Nagasaki and Yamaguchi, 1998; Baudoux and Brussaard, 2005; Tomaru *et al.,* 2005; Martínez-Martínez *et al*., 2015). Nevertheless, as viruses generally exhibit a broader thermotolerance than their hosts (Mojica and Brussaard, 2014), and because the optimal temperature for lytic replication (i.e. the temperature that generates fast host lysis and/or high viral yield) generally matches the host optimal growth temperature, it is usually assumed that the impact of temperature on viral infection mostly arises from changes in host metabolism. Temperature-driven changes in host physiology were indeed shown to alter the kinetics of viral lysis, possibly inducing the development of viral resistance (Nagasaki and Yamaguchi, 1998; Kendrick *et al*., 2014; Tomaru *et al*., 2014) or switches from a lysogenic to lytic lifestyle (Wilson *et al.,* 2001). Altogether, these studies point to important regulatory roles of temperature for viral infection. However, extrapolating results from culture studies to natural ecosystems remains risky given the paucity and the representativeness of the studied virus–host systems.

The cosmopolitan picophytoplankter *Micromonas* (Mamiellophyceae, Mamiellales) usually dominates the coastal eukaryotic phytoplankton communities from polar to tropical waters (Thomsen and Buck, 1998; Not *et al*., 2004; Foulon *et al.,* 2008; Balzano *et al*., 2012; Monier *et al*., 2015). Members of this prominent genus are distributed in three discrete genetic clades (Guillou *et al*., 2004; Foulon *et al*., 2008) that are all susceptible to viral infection (Baudoux *et al.,* 2015; Martínez-Martínez *et al*., 2015). Previous studies demonstrated that *Micromonas* viruses (MicVs) are ubiquitous, highly dynamic and induce substantial mortality through cell lysis events in natural and cultured populations (Cottrell and Suttle, 1991, 1995; Sahlsten, 1998; Zingone *et al*., 1999; Evans *et al.,* 2003; Baudoux *et al.,* 2015). The majority of known MicVs are lytic dsDNA viruses affiliated to the *Phycodnaviridae* family and the genus *Prasinovirus* (Mayer and Taylor, 1979; Cottrell and Suttle, 1991; Zingone *et al*., 2006; Martínez-Martínez *et al*., 2015), which may represent the most abundant viruses of eukaryotic marine plankton (Hingamp *et al.,* 2013; Yau *et al.,* 2015). *Micromonas* is among the phytoplankters that shows the widest latitudinal distribution on Earth and thereby inhabits waters with contrasted temperatures. Hence, *Micromonas*–virus system constitutes a particularly relevant biological model to investigate how temperature impacts host–virus interactions. To address this problem, we examined the thermal responses of three *Micromonas* strains that belong to the three main clades and three genetically distinct viruses and monitored the dynamics of the viral infection across a large thermal gradient.

Materials and methods

Algal and virus culture conditions

Micromonas sp. strains RCC451, RCC829 and RCC834 (hereafter referred to as Mic-A, Mic-B and

Table 1 *Micromonas* and virus strains used in this study

Clade	*Micromonas*			*Virus*					
	RCC #	*Strain name*[a]	*Isolation site and date*	*RCC #*	*Strain name*[a]	*Isolation site and date (mm/dd/yy)*	*Host range*[b]	*Latent period at 20 °C (hours)*[b]	*polB accession number*[b]
A	RCC451	Mic-A	*72.2 W 38.4 N 07/11/80*	RCC4253	MicV-A	*3.57 W 48.45 N 05/04/09*	Clade A	< 5	KP734133
B	RCC829	Mic-B	*14.3 E 40.7 N 01/08/97*	RCC4265	MicV-B	*3.57 W 48.45 N 09/28/09*	Clade A and B	*13*	KP734154
C	RCC834	Mic-C	*4.2 W 50.4 N 01/01/50*	RCC4229	MicV-C	*3.57 W 48.45 N 03/02/09*	Clade C	*24–27*	KP734144

Mic-A, Mic-B and Mic-C strains belong to *Micromonas* clade A, B and C, respectively.
[a]These denominations are used only in this study.
[b]These informations are from Baudoux *et al.* (2015).

Mic-C; Table 1) that belong to the phylogenetic clades A, B and C, respectively, were retrieved from the Roscoff Culture Collection (http://roscoff-culture-collection.org/). Algal cultures were grown in batch conditions in ventilated polystyrene flasks (Nalgene, Rochester, NY, USA) in K-Si medium (Keller *et al.*, 1987). Cultures were maintained under 100 μmol photons m^{-2} s^{-1} of white light provided by fluorescent tubes (Mazda 18WJr/865) using a 12:12 light:dark cycle in temperature-controlled chambers at 4, 7.5, 9.5, 12.5, 20, 25, 27.5, 30 and 32.5 °C (Aqualytic, Dortmund, Germany). Cultures were thermo-acclimated for several months by multiple serial transfers of early exponentially growing cells.

Viral strains RCC4253, RCC4265 and RCC4229 (hereafter referred to as MicV-A, MicV-B and MicV-C) that are lytic to *Micromonas* Mic-A, Mic-B and Mic-C, respectively, were chosen based on the characterization conducted in Baudoux *et al.* (2015) (Table 1). Viral lysates were produced by infecting host cultures grown at 20 °C. The model system Mic-B/MicV-B was explored in detail because of its large thermal range.

Flow cytometry

All flow cytometric analyses were carried out using a flow cytometer FACS Canto II (Becton Dickinson, San Jose, CA, USA) equipped with an air-cooled argon laser at 488 nm. Green fluorescence intensity (530 nm emission), red fluorescence intensity (emission >660nm), side scatter and forward scatter were normalized with standard 0.95 μm fluorescent beads (YG, Polysciences, Warrington, PA, USA).

Micromonas cell abundances (Figure 1a) were determined using the side scatter and the red fluorescence signals. The samples were analysed for 1 min at the appropriate flow speed according to culture concentration in order to avoid coincidence events (Marie *et al.*, 1999). The growth rates of *Micromonas* Mic-A, Mic-B and Mic-C acclimated from 4 to 30 °C were computed as the slope of ln(*Nt*) vs time plot, where *Nt* is the cell number at time *t*. All measurements were done on at least four replicates.

In addition, cell membrane permeability, used as a proxy for viability, was monitored by flow cytometry using SYTOX-Green. This dye is a membrane-permeant nucleic acid probe (Life Technologies, Saint-Aubin, France) that only binds to nucleic acids of cells that have comprised membranes. SYTOX-Green (0.5 μM final concentration) was added to fresh sample, and the mixture was incubated for 5 min in the dark at the corresponding growth temperature (Peperzak and Brussaard, 2011). Cells with compromised membranes were discriminated based on their higher green fluorescence (Figure 1b).

Viral abundances were determined on glutaraldehyde-fixed samples (0.5% final concentration, Grade II; Sigma Aldrich, St Louis, MO, USA) stored at −80 °C until analysis. Flow cytometry analysis was performed as described by Brussaard (2004). Briefly, samples were thawed at 37 °C, diluted in 0.2 μm filtered autoclaved TE buffer (10:1 Tris-EDTA, pH = 8) and stained with SYBR-Green I (concentration; Life Technologies, Saint-Aubin, France) for 10 min at 80 °C. Virus particles were discriminated based on their green fluorescence and side scatter during 1 min analyses (Figure 1c). All cytogram analyses were performed with the Flowing Software freeware (Turku Center of Biotechnology, Turku, Finland).

Micromonas growth rate modelling

A Cardinal Temperature Model with Infection relying on experimental growth rates was used to calculate the optimal growth temperature (T_{opt}), for which growth rate is optimal (μ_{opt}), and the minimal and maximal growth temperatures (T_{min} and T_{max}) beyond which growth rate is assumed to be zero (Bernard and Rémond, 2012). The determination of these parameters was essential to select the appropriate temperature for infection experiments. Cardinal temperatures (T_{min}, T_{opt} and T_{max}) of *Micromonas* and thermal growth response were predicted using the relation:

$$\mu_{max} = \begin{cases} 0 \text{ for } T < T_{min} \\ \mu_{opt} \cdot \phi(T) \text{ for } T_{min} < T < T_{max} \\ 0 \text{ for } T > T_{max} \end{cases}$$

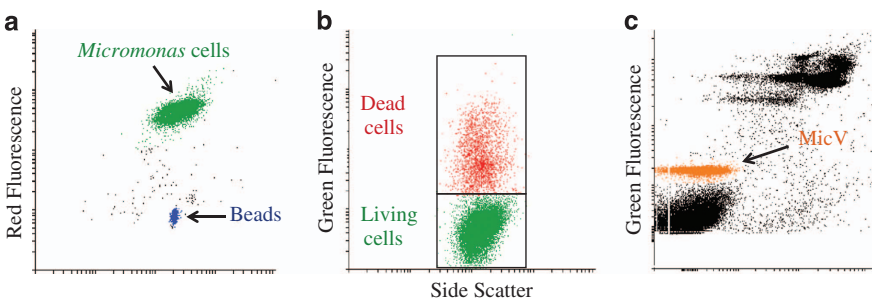

Figure 1 Flow cytograms representing (**a**) *Micromonas* cells discriminated using the red fluorescence and the side scatter channels for total cell enumeration, (**b**) *Micromonas* membrane integrity upon SYTOX-Green staining which discriminates dead cells and live cells based on the green fluorescence channel. (**c**) MicV particles discriminated by their green fluorescence and side scatter channels upon staining with the nucleic acid dye SYBR-Green.

where

$$\phi(T) = \frac{(T - T_{max})(T - T_{min})^2}{(T_{opt} - T_{min})[(T_{opt} - T_{min})(T - T_{opt}) - (T_{opt} - T_{max})(T_{opt} + T_{min} + 2T)]}$$

The same algorithm was used in Bernard and Rémond (2012) to identify model parameters and the confidence intervals were determined with a jackknife method with a 95% threshold.

Pulse amplitude modulated fluorimetry

The quantum yield of photosystem II of algal cells was determined using a pulse amplitude modulated fluorometer (Phyto-PAM, Walz) connected to a chart recorder (Labpro; Vernier) in order to monitor the impact of temperature and viral infection on host photophysiology. After 5 min relaxation in darkness, the non-actinic modulated light (450 nm) was turned on in order to measure the fluorescence basal level, F_0. A saturating red light pulse (655 nm, 4000 μmol quanta m^{-2} s^{-1}, 400 ms) was applied to determine the maximum fluorescence level in the dark-adapted sample, F_M. The maximal photosystem II fluorescence quantum yield of photochemical energy conversion, F_V/F_M, was calculated using the following formula:

$$\frac{F_V}{F_M} = \frac{(F_M - F_0)}{F_M}$$

Measuring the effect of temperature on virion infectivity and abundance

Freshly produced 0.2 μm filtered (polyethersulfone membrane) viral lysates of MicV-A, MicV-B and MicV-C were diluted in K-Si culture medium to a final concentration of 10^6 viral particles ml^{-1}. Aliquots of these viral suspensions were incubated in darkness at 4, 7.5, 12.5, 20, 25, 27.5, 30 °C, which corresponds to the global temperature range encountered in the ocean. Samples for total virus abundance and infectivity were taken once a week and once every 2 weeks, respectively, during 6 weeks. Viral abundance was monitored by flow cytometry as described above. Viral infectivity was assessed using end point dilution method (Most Probable Number (MPN) method; Taylor, 1962). To this end, virus suspensions were serially diluted (10-fold increments) in exponentially growing *Micromonas* cultures in 48-multiwell plates and incubated at 20 °C for 10 days. Each serial dilution was done in triplicate along with a control, non-infected *Micromonas* culture. After incubation, the cultures that underwent lysis, as seen by the colour change, were counted and the infectious virus concentration was determined with the software *Most Probable Number* (MPN; version 2.0; Avineon, U.S Environmental Protection Agency).

Particle degradation and decrease in infectivity rates (respectively d_S and d_i) were calculated from viral counts and viral infectivity measurements as follows:

$$d_s = \frac{\ln(V_{t+1}) - \ln(V_t)}{t_{+1} - t}$$

where V_{t+1} and V_t are the concentration of viral particles at time t_{+1} and t, respectively, and

$$d_i = \frac{\ln(I_{t_{+1}}) - \ln(I_t)}{t_{+1} - t}$$

where I_{t+1} and I_t are the concentrations of infectious viral particles at time t_{+1} and t, respectively.

Measuring the effect of temperature on the Micromonas*–virus interactions*

The effects of temperature on virus–host interactions were assessed by infection dynamics experiments. For the model system Mic-B/MicV-B, host cultures acclimated at 9.5, 12.5, 20, 25, 27.5 and 30 °C were prepared at a concentration of 5×10^5 cell ml^{-1} and split into four subcultures. Three of the subcultures were infected with a fresh, 0.2 -μm-filtered virus lysate of MicV-B at a multiplicity of infection of 10. The fourth culture, uninfected, served as control. Control and infected cultures, incubated at each temperature, were sampled every 3–4 h during 120 h for measurements of host and viral abundances, host cell membrane integrity and photosynthetic capacity (see above).

Three viral parameters, the latent period, the viral production and, when applicable, the burst size, were calculated from viral growth cycle. The latent period was calculated as the lapse-time between inoculation of viruses in host culture and the release of viral particles by host cells. A viral production rate was calculated as the slope of the logarithm curve of viral concentration over time following the equation:

$$\text{viral production rate} = \frac{\ln(V_{t+1}) - \ln(V_t)}{\Delta_t}$$

with V_{t+1} the viral concentration at time t_{+1} and V_t the viral concentration at time t for the period $\Delta_t = t_{+1} - t \leqslant 24$ h.

If complete host lysis occurred, the burst size (BS) was calculated as the number of viral particles produced per infected host cell as

$$BS = \frac{V_{max} - V_0}{H_{max} - H_{min}}$$

where V_0 is the viral concentration and T_o, V_{max} the maximum concentrations of viral particles during the experiment, and H_{max} and H_{min} the maximal and minimal host abundances during the experiment.

For the model systems Mic-A/MicV-A and Mic-C/MicV-C, a simplified experimental setup and sampling strategy were used. Infection cycles were monitored at only five temperatures: 12.5, 20, 25, 27.5 and 30 °C. Infections at 12.5, 20, 27.5 and 30 °C

were sampled every 10–14 h during 120 h for host and virus abundance and photosynthetic capacity measurements. Infections at 25 °C were sampled for host and virus abundance every 3–4 h during 28 h and every 12 h for the remaining 96 h.

Results

Effect of temperature on Micromonas *growth*

The growth rate of *Micromonas* sp. strains Mic-A, Mic-B and Mic-C was measured at temperatures ranging from 4 to 32.5 °C (Figure 2; Table 2). The growth responses to temperature followed a typical, asymmetric bell-shaped curve over the selected temperature range with an asymptotic increase at temperatures below T_{opt} and an abrupt decline at temperatures beyond $T_{opt.}$ Cardinal Temperature Model with Infection model fitting resulted in the determination of optimum growth temperature (T_{opt}) values of 25.1, 26.7 and 24.3 °C for Mic-A, Mic-B and Mic-C, respectively. Mic-A and Mic-C showed a similar optimal growth rate ($\mu_{opt} = 0.8\ day^{-1}$), while Mic-B ($\mu_{opt} = 1.1\ day^{-1}$) was higher. *Micromonas* strain Mic-B exhibited the largest thermal range with a theoretical T_{min} of 0.55 °C and T_{max} of 32.5 °C.

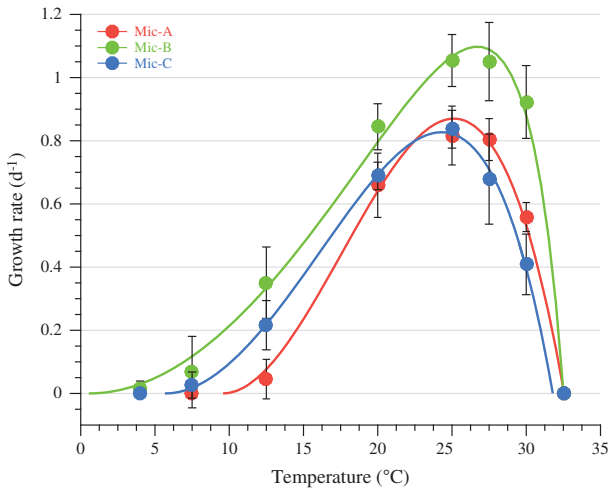

Figure 2 Growth response to temperature of *Micromonas* sp. strains Mic-A (red), Mic-B (green) and Mic-C (blue). Closed circles represent experimental data and solid lines indicate the fit of the Cardinal Temperature Model with Infection model from Bernard and Rémond (2012). Error bars represent the standard deviation of the data (at 95%, at least $n = 3$).

Mic-A and Mic-C appeared slightly more restrictive with a positive growth between 9.6 and 32.5 °C and 5.7–30.1 °C, respectively. Based on these thermal responses, we investigated the stability of the virus particles and the potential changes in the virus–host interactions below or at T_{opt} (7.5 or 9.5, 12.5, 20 and 25 °C) and beyond T_{opt} (27.5 and 30 °C).

Thermal stability of Micromonas *virions*

The thermal stability of the viral particles MicV-A, MicV-B and MicV-C was investigated over a 6-week period, during which viral infectivity and particle integrity were monitored. Rates of decay for these two parameters varied considerably among the three viral strains (Figure 3). MicV-C was the most stable over the range of selected temperature. MicV-C infectivity and particle integrity both declined at similar rates between 7.5 °C ($0.08 \pm 0.05\ day^{-1}$) and 27.5 °C ($0.1 \pm 0.02\ day^{-1}$), while infectivity decay rates increased considerably only at 30 °C ($0.35 \pm 0.02\ day^{-1}$). The infectivity decay rates were globally higher for MicV-A and MicV-B virions, increasing gradually (from 0.17 ± 0.025 to $0.44 \pm 0.01\ day^{-1}$) with increasing temperature. In spite of these considerable losses in infectivity, total counts of viral particles decreased at much lower rates, suggesting that MicV-A and MicV-B had lost the ability to infect their hosts prior to particle destruction.

Impact of temperature on virus–host interactions

Infection dynamics experiments revealed that virus–host interactions were strongly affected by temperature, but each virus–host systems displayed distinct responses (Figures 4 and 6).

Mic-B/MicV-B

Both infection kinetics and the fate of the infected *Micromonas* cells differed between temperature treatments. Below Mic-B T_{opt} (25, 20, 12.5 and 9.5 °C), MicV-B propagated through a typical lytic cycle (Figure 4). The virus latent period increased progressively with decreasing temperature ranging from <3 h at 25 °C to the 7–11 h at 12.5 and 9.5 °C (Figures 4a–d). Similarly, the rates of virus production were substantially faster at 25 and 20 °C (5.76 and $5.52\ day^{-1}$; Figures 4c and d) compared with that at 9.5 and 12.5 °C (0.48 and 0.96 virus

Table 2 Cardinal temperatures (°C), optimal growth rates (day^{-1}) and their respective confidence intervals (CI_{low} and CI_{up}) for the three *Micromonas* strains

Micromonas strains	*Mic-A*	*Mic-B*	*Mic-C*
T_{min} ($CI_{low} - CI_{up}$)	9.6 (7.5 to 11.5)	0.55 (–2.3 to 3.3)	5.7 (3.3 to 7.9)
T_{opt} ($CI_{low} - CI_{up}$)	25.1 (24.5 to 25.8)	26.7 (25.9 to 27.5)	24.3 (23.4 to 25.2)
T_{max} ($CI_{low} - CI_{up}$)	32.6 (32.4 to 32.7)	32.5 (32.49 to 32.53)	31.8 (30.3 to 33.2)
μ_{opt} ($CI_{low} - CI_{up}$)	0.87 (0.82 to 0.92)	1.1 (1.05 to 1.15)	0.83 (0.76 to 0.87)

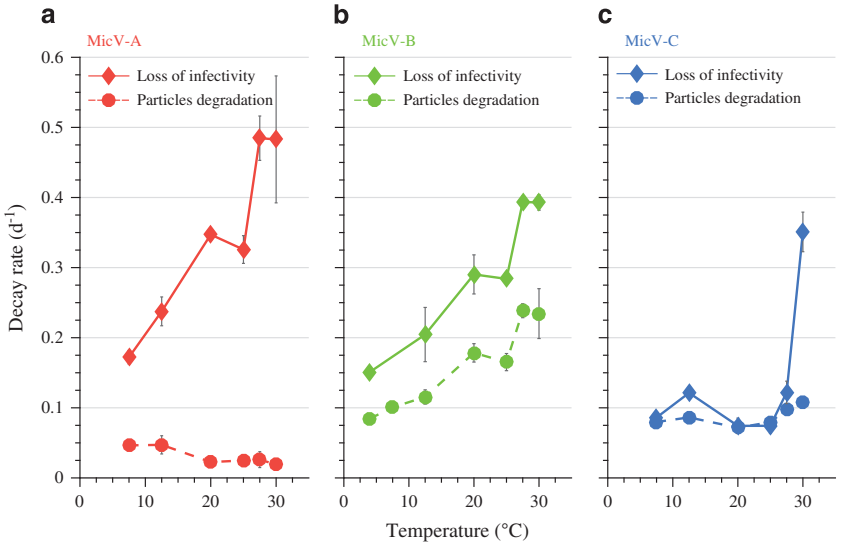

Figure 3 Decay rates of viral particles (dashed line) and viral infectivity (solid line) for MicV-A (**a**), MicV-B (**b**) and MicV-C (**c**) exposed to a large range in temperatures over a 6-week incubation period. Error bars represent the confidence intervals (at 95%, $n = 3$).

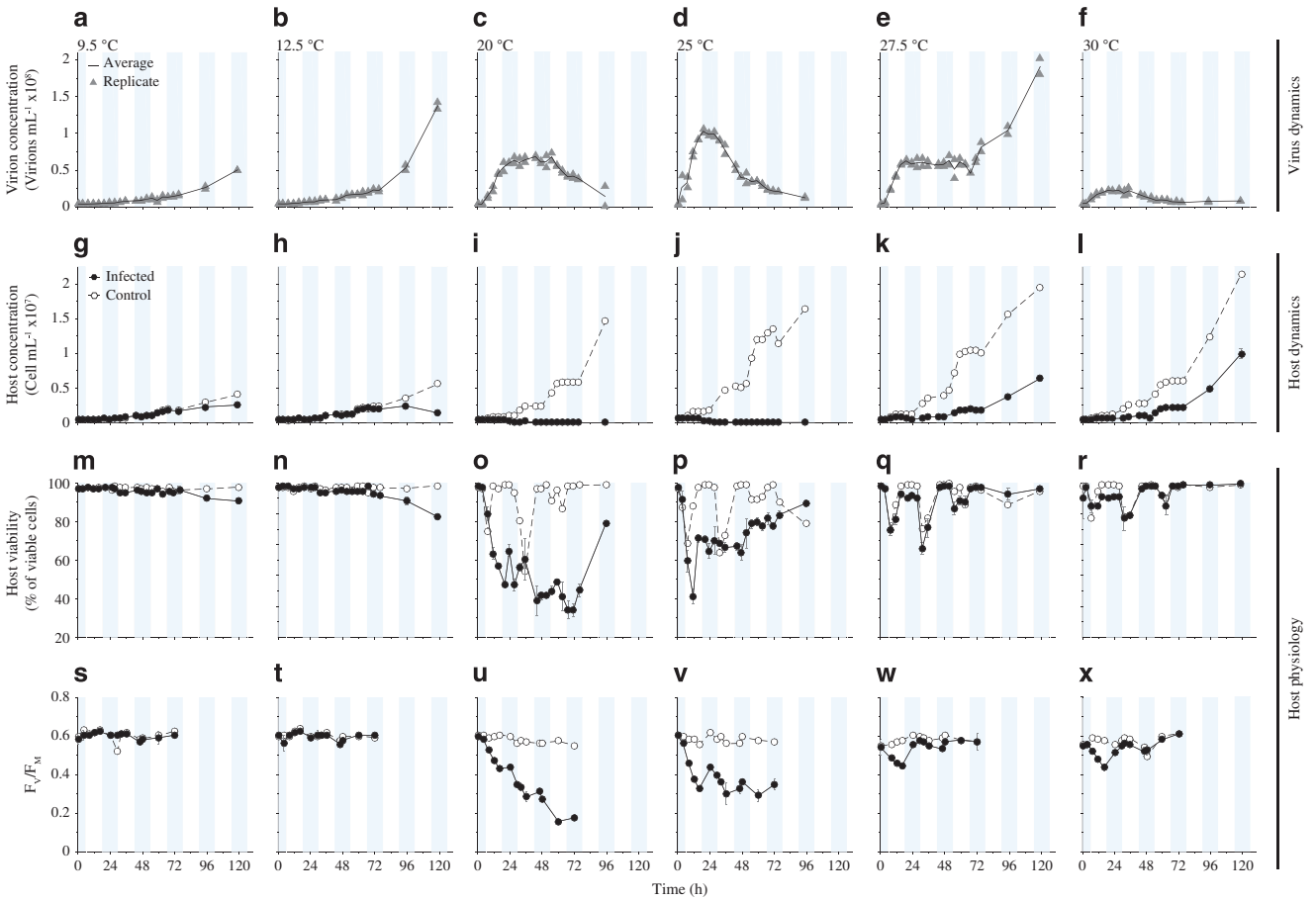

Figure 4 Viral infection of *Micromonas* Mic-B by MicV-B at 9.5, 12.5, 20, 25, 27.5 and 30 °C. Dynamics of viral abundance (panels **a–f**, data in grey triangles and mean of two replicates in black lines), *Micromonas* abundance (panels **g–l**) in control (dashed lines and white circles) and infected (solid lines and black circles) cultures, % cells with intact membranes (viable cells, panels **m–r**) in control (dashed lines and white circles) and infected (solid lines and black circles) cultures, and photosynthetic capacity (panels **s–x**) of control (dashed lines and white circles) and infected (solid lines and black circles) cultures are shown. Blues bars represent the light phases. Error bars were computed from triplicate samples for the host parameters. Virus particles were enumerated from duplicate samples, so no error bar is shown.

produced day^{-1}, respectively, Figures 4a and b). The virus production at 25 and 20 °C induced host cell lysis, which was accompanied by a disruption of host membranes (Figures 4o and p and Supplementary Figure S1) and a decrease in photosynthetic capacity (Figures 4u and v). The resulting burst size (139 to 142 virions host^{-1}) was comparable for both temperature treatments. At 12.5 and 9.5 °C, the host cell lysis was delayed considerably. At these temperatures, control and infected cultures displayed similar growth rates (Figures 4g and h) and neither the host membrane integrity (Figures 4m and n) nor the photosynthetic capacity (Figures 4s and t) appeared to be altered by the virus production until 70 h post infection. The loss in host abundance recorded 70 h post infection (Figures 4g and h) led to estimate a burst size of 84 virions host^{-1} at 12.5 °C. At 9.5 °C, the infected host abundance did not decline during the 120 h sampling, precluding calculation of the burst size. Lysis of infected host was nevertheless confirmed by a visual control (the infected culture became transparent) at 140 h post infection.

At temperatures above T_{opt} (27.5 and 30 °C), complete host cell lysis was not observed and viral infections appeared to follow a two-step process. At 27.5 °C, virus infection led to a rapid release of viral progeny (latent period <3 h) at a substantial production rate (6.24 day^{-1}) until a plateau in virus concentration was reached after 20 h (Figure 4e). A second increase in viral abundance with a production rate of 0.48 day^{-1} was recorded after 70 h, which was maintained until the end of the experiment. Interestingly, viral infection at 27.5 °C did not result in complete collapse of the host culture (Figure 4k and Supplementary Figure S1). A slight decline in infected host cell abundance (Figure 4k), membrane integrity (from 100% to 90%; Figure 4q) and F_V/F_M (from 0.55 to 0.45; Figure 4w) accompanied the first viral burst (BS of 177 virions host^{-1}). However, the second production of viruses did not induce cell lysis. Indeed, infected host cells grew at slower rates than control cultures (0.62 day^{-1} compared with 1.11 day^{-1}; Figure 4k), yet they exhibited unaltered membrane integrity (Figure 4q) and F_V/F_M (Figure 4w) compared with the control. The estimation of the viral BS was not possible in the absence of a host cell lysis; instead we calculated a viral release of 5 virions cell^{-1} day^{-1}.

Last, virus infection at 30 °C resulted in a reduced production rate of viral progeny (3.6 day^{-1}) after a latent period of 3–7 h and a gradual decay in viral abundance from 35 h until the end of the experiment (Figure 4f). As observed at 27.5 °C, the viral production was accompanied by an incomplete host cell lysis (Figure 4l and Supplementary Figure S1). The production of viral progeny and subsequent cell lysis induced slight declines in infected host cell abundance, membrane integrity (from 100% to 90%; Figure 4r) and F_V/F_M (from 0.55 to 0.45; Figure 4x). The resulting viral BS reached 49 virions host^{-1}.

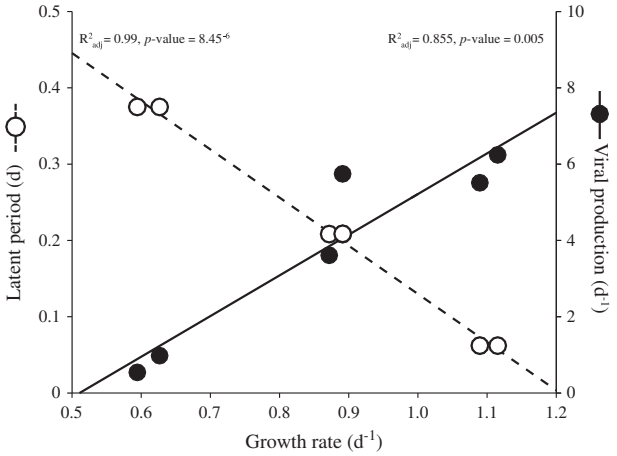

Figure 5 Relationship between viral latent period (dashed line and white circle), viral production (solid line and black circle) and host growth rate for the system Mic-B/MicV-B. Linear regressions were statistically robust with an adjusted $R^2 > 0.85$ and a P-value < 0.05.

Yet, we observed a regrowth of infected host at a rate of 0.81 day^{-1} (compared with 0.69 day^{-1} for the control) after 80 h (Figure 4l) and restoration of membrane integrity and photosynthetic capacity after 27 h until the end of the experiment (Figures 4r and x).

Altogether, these results indicate that rates of viral production were positively related to host growth rate whereas viral latent period was inversely related to the host growth rates (Figure 5). Optimal viral replication (shortest latent period and fastest viral production) occurred at a temperature between 25 and 27.5 °C, which correspond to the optimal growth of *Micromonas* Mic-B.

Mic-A/MicV-A and Mic-C/MicV-C

As observed for MicV-B, MicV-A and MicV-C replicated through a typical lytic cycle only below host T_{opt} (20 and 12.5 °C; Figure 6). At 20 °C, viruses were released after latent periods lower than 14 h and 14–24 h for MicV-A and MicV-C, respectively, with virion production rates of 2.64 day^{-1} and 1.44 day^{-1}, respectively. The strong decrease in cell abundance in the infected cultures indicates that viral production induced complete collapse of the corresponding host culture (Figure 6g and Supplementary Figure S2). The resulting BS reached values of 130–158 virions host^{-1} and 177–197 virions host^{-1} for MicV-A and MicV-C, respectively (Figure 6b). At 12.5 °C, MicV-A and MicV-C readily propagated in their respective host; yet the duration of virus latent periods were prolonged (19–29 h) compared with the 20 °C treatment with virion production rates of 1.2 and 0.96 day^{-1}, respectively (Figure 6a). The release of viral progeny was accompanied by immediate host lysis and the resulting burst size was reduced for MicV-A and MicV-C (57–69 and 80–96 virions host^{-1},

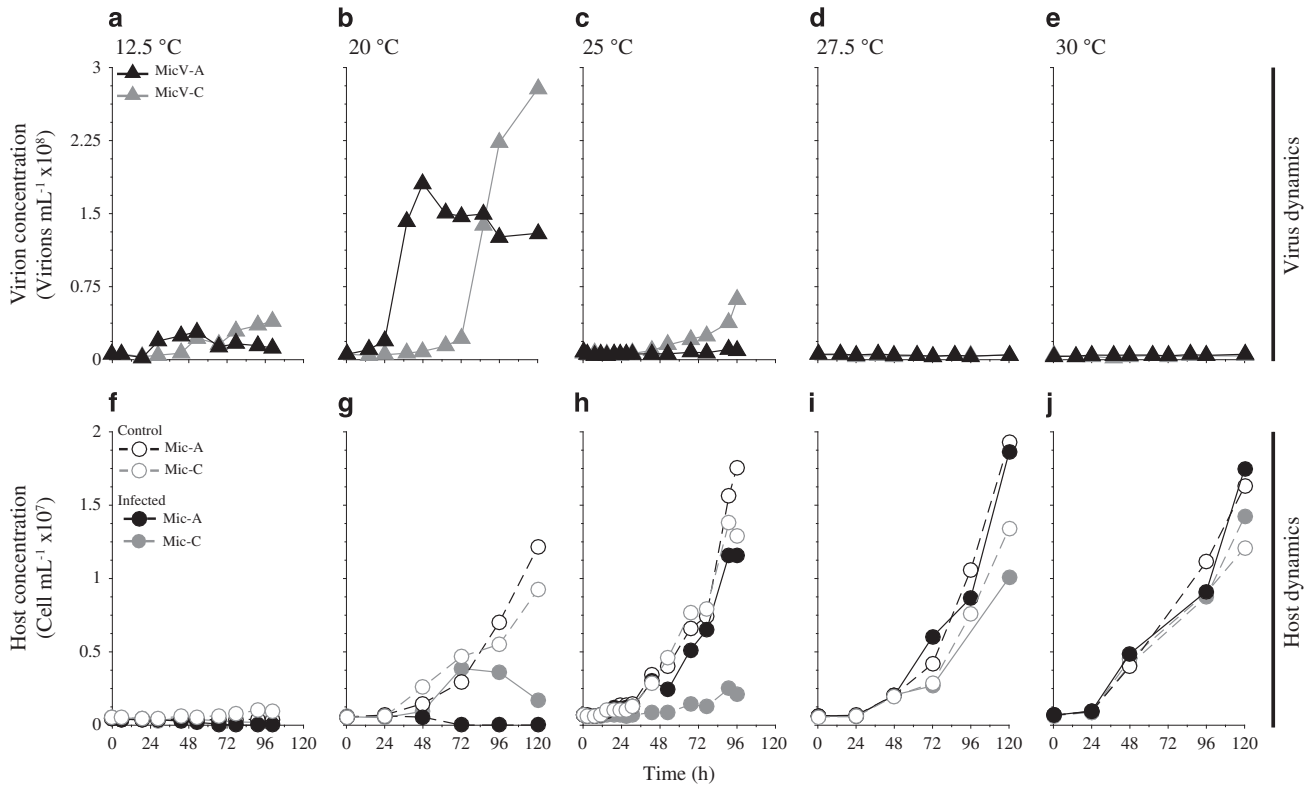

Figure 6 Viral infection of *Micromonas* Mic-A by MicV-A (black symbols and lines) and *Micromonas* Mic-C by MicV-C (grey symbols and lines) at 12.5, 20, 27.5 and 30 °C. Dynamics of virus abundance (**a**–**e**) for MicV-A (black triangles) and MicV-C (grey triangles) are shown in the upper panels. Dynamics of *Micromonas* abundance (**f**–**j**) for Mic-A in control (black open circles and dashed lines) and infected cultures (black circles and solid lines) and Mic-C in control (grey open circles and dashed lines) and infected cultures (grey circles and solid lines) are shown in the bottom panels.

respectively) compared with infection at 20 °C (Figure 6f and Supplementary Figure S2).

At temperatures close to T_{opt} (25 °C), infection by MicV-A and MicV-C did not result in cell lysis while viruses were still produced (Figures 6c and h and Supplementary Figure S2). The duration of the virus latent periods was similar (7–11 and 27–31 h) compared with the 20 °C treatment with virion production rates of 0.48 and 0.84 day^{-1}, respectively. The resulting growth rate of infected Mic-A cells was not different to the control (0.8 day^{-1}) whereas infected Mic-C grew at a lower rate than the control (0.36 vs 1.02 day^{-1}).

At temperatures beyond host T_{opt} (27.5 and 30 °C), infection by MicV-A and MicV-C did not result in any production of viruses. Infected *Micromonas* cells were apparently not altered by the presence of viruses, growing at rates similar to control cultures (Figures 6d, e, i and j) with unaffected photosynthetic yields (data not shown).

Discussion

The response of *Micromonas* strains to temperature is typical for a eurythermal mesophilic species, characterized by a wide range of thermal tolerance with an optimal growth temperature (T_{opt}) between 20 and 25 °C. Deviation from the optimal growth temperature is thought to induce modifications of intrinsic biochemical and physiological functions in order to optimize resource allocation for growth on the one hand, and to maintain cell integrity on the other hand (Behrenfeld *et al*., 2008; Ras *et al*., 2013). As a result, *Micromonas* growth response below T_{opt} reflects cold acclimation whereas the abrupt decline of growth rates beyond T_{opt} suggests dramatic deleterious effects of heat on cellular components (Raven and Geider, 1988; Dill *et al*., 2011; Ras *et al*., 2013). Although the three *Micromonas* strains exhibited broad temperature tolerances, the strain belonging to clade B (Mic-B) showed the largest thermal tolerance range (from 0.55 to 32.5 °C) while strains belonging to clades A and C were more restrictive with thermal tolerance ranging from 9.6 to 32.5 °C and from 5.7 to 30.1 °C, respectively. Whether these differences are generally the case for all of the members of these clades remains to be investigated. To the best of our knowledge, no study has explored the existence of thermotypes in *Micromonas* species. Nonetheless, our results suggest that the selected *Micromonas* strains might have evolved divergent acclimation strategies, which may, in turn, influence virus–host interactions.

The detailed study of the model system Mic-B/MicV-B unequivocally demonstrated that

viral infection is altered by temperature. At temperatures lower than T_{opt}, MicV-B propagated and killed their hosts through cell lysis as classically reported in the literature (Mayer and Taylor, 1979; Zingone *et al.*, 2006; Baudoux *et al.*, 2015; Martínez-Martínez *et al.*, 2015). Yet the kinetics and the intensity of viral replication slowed down with decreasing temperatures. MicV-B propagated the most efficiently at 25 °C, which corresponded to a temperature close to the optimal growth temperature of *Micromonas* sp. Mic-B. Under these growth conditions, MicV-B readily adsorbed on host membranes and rapidly hijacked host cellular machinery for viral DNA replication as well as virion protein synthesis and assembly, as indicated by the short latent period (<3 h), the high burst size (140 virions per infected cell) and the fast viral production rate (5.5 day^{-1}). The observed viral parameters fall within the range of reported values for other *Micromonas* viral isolates (Mayer and Taylor, 1979; Baudoux and Brussaard, 2008; Baudoux *et al.*, 2015). Decrease in temperature led to increased latent periods and the coldest temperatures (12.5 and 9.5 °C) also induced a reduction of viral production rates and a substantial delay in host cell lysis. The relatively low viral decay rates recorded across this thermal range indicated that MicV-B particles did remain infectious under these conditions. It is thus likely that the acclimation strategy evolved by Mic-B to grow at temperatures below T_{opt} was responsible for the alteration of the viral infection process. The decrease in auto-fluorescence intensity of cold-adapted *Micromonas* (Supplementary Figure S3) suggests a reduction in chlorophyll content with decreasing temperatures as previously reported (Claquin *et al.*, 2008). Several studies pointed out the similarity of photoacclimation trends at low temperatures to those at high irradiance (Anning *et al.*, 2001; El-Sabaawi and Harrison, 2006; Claquin *et al.*, 2008). Reports on the effect of light intensity evidenced the importance of this factor in regulating algal host–virus interactions (Waters and Chan, 1982; Bratbak *et al.,* 1998; Brown *et al.*, 2007; Baudoux and Brussaard, 2008). However, elevated irradiance *per se* did not appear to alter viral infection of *Micromonas* (Baudoux and Brussaard, 2008). Several other reasons might explain changes in viral infection of Mic-B at low temperatures. For example, low temperatures were shown to slow down the rates of translation initiation at the ribosome site in phytoplankton (Toseland *et al.,* 2013). The globally reduced metabolic activities and protein biosynthesis may thus result in a slower synthesis and assembly of virions proteins, which, in turn, could explain the decrease in viral progeny production. Another known impact of low temperatures is the stiffening of phytoplankton membranes through the activation of lipid desaturases (Los and Murata, 2004; D'Amico *et al.*, 2006). Interestingly, the monitoring of *Micromonas* membrane integrity indicated a modification of their membrane properties. While cell division enhanced membrane permeability at 25 and 20 °C, host membranes remained impermeable to the dye throughout their cell cycle at the coldest temperatures (9.5 and 12 °C), supporting the idea that Mic-B membranes became more rigid. Such modification might not only impact viral adsorption on host cell, which would result in a prolonged latent period, but it may also delay the release of viral progeny and, thereby, the timing of host lysis.

Notably, temperatures above T_{opt} altered the algicidal activity of *Micromonas* viruses considerably. A 1 °C temperature increase beyond T_{opt} induced host tolerance to viral infection. At 27.5 °C, we indeed observed a rapid transition from a classical lytic infection mode to a viral life strategy reminiscent of chronic infection, by which viruses are released with no apparent sign of host lysis. This infection mode has never been reported in MicV. Yet, one of the few examples of chronic infection in marine systems has interestingly been described for another prasinovirus that infects the green alga *Ostreococcus tauri*, a close relative of *Micromonas* sp. (Thomas *et al.*, 2011). *Ostreococcus* virus OtV-5 switched from a lytic to a chronic lifestyle within a few days of incubation, after lysis of most of the host cells remaining host cells were resistant but produced viruses chronically. The viral yield of chronically infected cells is within the same range for both model systems with 1–3 and 5 viruses $host^{-1}$ day^{-1} in *Ostreococcus* and *Micromonas*, respectively. Yet, the growth rate of chronically infected *Micromonas* cells was considerably reduced while no reduction in growth rate was evidenced in *Ostreococcus* species (Thomas *et al.*, 2011). As argued for lysogeny, chronic infection ensures a coexistence between host and virus in unfavourable conditions (e.g. low host density, suboptimal growth environments, Mackinder *et al.*, 2009; Thomas *et al.*, 2012). Being in the vicinity of their host may directly benefit the virus if growth conditions improved. The mechanisms that trigger a lytic–chronic decision remain to be established. Our results however suggest that this switch in life strategy did not operate when temperatures deviated excessively from the growth optimum. At 30 °C, MicV-B rapidly replicated through cell lysis and regrowth of infected *Micromonas* cells was recorded following this lytic event as observed at 27.5 °C. A number of interpretations could explain the findings of low viral production and continued host growth at 30 °C. The observed loss of viral infectivity at this temperature suggests that viruses could become inactive during the period of the experiment. However, we cannot rule out that alterations of host phenotype modify their susceptibility to viral infection as demonstrated recently in Kendrick *et al.* (2014). Hence, temperatures above T_{opt} induced complex outcomes after viral infection in Mic-B. Importantly, chronic infections might arise more frequently than previously thought, at least among marine prasinophytes.

The investigation of two additional Micromonas–virus systems suggests that the previously observed temperature effects on the viral infection process are not specific to the model system Mic-B/MicV-B. Despite the variable thermal tolerance of the studied *Micromonas* hosts and their respective viruses, temperature affected the outcome of viral infections similarly. Infection dynamics experiments demonstrated that temperatures below T_{opt} slowed down the kinetics and intensity of the lytic cycle while temperatures close to and higher than T_{opt} induced complex outcomes in viral infections. Infections at 25 °C might correspond to temperature slightly above T_{opt} as the averaged predicted T_{opt} were 25.1 °C (24.5–25.8) and 24.3 °C (23.4–25.2) for Mic-A and Mic-C, respectively. As observed previously, a slight increase beyond T_{opt} induced a viral life strategy reminiscent of chronic infection while excessive deviation from T_{opt} inhibited viral production, although hosts maintained their ability to grow. Hence, the thermal environment of *Micromonas* determines the outcome of viral infection, leading to drastic changes in the lytic cycle and a possible switch in viral life strategy. Similar thermal responses to viral infection were reported for the raphidophyte *Heterosigma akashiwo* (Nagasaki and Yamaguchi, 1998) and the haptophyte *Emiliania huxleyi* (Kendrick *et al*., 2014). An alteration of the algicidal activity of viruses at high temperatures and a reduced intensity of viral lysis at low temperatures seem to represent a global pattern, which may have important consequences for the regulation of phytoplankton population in the ocean.

Because of their worldwide distribution and persistence in marine systems, *Micromonas* and their viruses are exposed to important changes in environmental parameters, including temperature. Results of this study clearly demonstrated that a 1 °C change can profoundly affect the outcome of viral infection and can even lead to development of complex outcomes of viral lysis. It is thus very likely that temperature contributes to the control of viral induced mortality in *Micromonas* populations both at a temporal and a geographical scale. There is, to our knowledge, no report of actual viral lysis rates in *Micromonas* natural populations to support our speculation. Nonetheless, a recent study observed a latitudinal variation in virus-mediated mortality of phytoplankton across the North Atlantic Ocean and pointed out a correlation between the velocity of viral lysis and *in situ* temperature that varied between 10 and 25 °C (Mojica *et al*., 2015). Such geographic partitioning of viral lysis processes could have important consequences for the ecology and the biogeochemistry of the global ocean. Viral lysis diverts phytoplankton biomass away from the higher trophic level towards the microbial loop through the release of cellular compounds upon host cell lysis. Temperature-driven changes in the amount of viral-mediated mortality and in host cell stoichiometry (due to changes in biochemical functions) could thereby alter the structure of marine food webs and the capacity of pelagic systems to sequester carbon. Given the anticipated increase of sea surface temperature due to global warming, it is essential to gain a better understanding of the thermal response and life strategy in other prominent virus–phytoplankton model systems. Such studies are necessary for improving ecosystem models in ecosystem-based considerations of climate change.

Conflict of Interest

The authors declare no conflict of interest.

Acknowledgements

We are grateful to the MICROBIOL Master students 2015–2016 for repeating infection dynamics experiments and to Nigel Grimsley, Hervé Moreau and Evelyne Derelle for stimulating discussions. We thank the three anonymous reviewers for their constructive comments on a previous version of this manuscript. This research was funded by the ANR funding agency REVIREC; grant no. 12-BSV7-0006-01.

References

Anning T, Harris G, Geider R. (2001). Thermal acclimation in the marine diatom Chaetoceros calcitrans (Bacillariophyceae). *Eur J Phycol* **36**: 233–241.

Balzano S, Marie D, Gourvil P, Vaulot D. (2012). Composition of the summer photosynthetic pico and nanoplankton communities in the Beaufort Sea assessed by T-RFLP and sequences of the 18S rRNA gene from flow cytometry sorted samples. *ISME J* **6**: 1480–1498.

Baudoux A-C, Brussaard CPD. (2005). Characterization of different viruses infecting the marine harmful algal bloom species Phaeocystis globosa. *Virology* **341**: 80–90.

Baudoux A-C, Brussaard CPD. (2008). Influence of irradiance on virus-algal host interactions. *J Phycol* **44**: 902–908.

Baudoux A-C, Lebredonchel H, Dehmer H, Latimier M, Edern R, Rigaut-Jalabert F *et al*. (2015). Interplay between the genetic clades of Micromonasand their viruses in the Western English Channel. *Environ Microbiol Rep* **44**: 765–773.

Behrenfeld MJ, Halsey KH, Milligan AJ. (2008). Evolved physiological responses of phytoplankton to their integrated growth environment. *Philos Trans R Soc B* **363**: 2687–2703.

Bernard O, Rémond B. (2012). Validation of a simple model accounting for light and temperature effect on microalgal growth. *Bioresour Technol* **123**: 520–527.

Bratbak G, Heldal M, Thingstad TF, Riemann B, Haslund OH. (1998). Viral lysis of *Phaeocystis pouchetii* and bacterial secondary production. *Aquat Microb Ecol* **16**: 11–16.

Brown CM, Campbell DA, Lawrence JE. (2007). Resource dynamics during infection of Micromonas pusilla by virus MpV-Sp1. *Environ Microbiol* **9**: 2720–2727.

Brum JR, Sullivan MB. (2015). Rising to the challenge: accelerated pace of discovery transforms marine virology. *Nat Rev Microbiol* **13**: 147–159.

Brussaard CPD. (2004). Viral control of phytoplankton populations—a review. *J Eukaryot Microbiol* **51**: 125–138.

Brussaard CP, Wilhelm SW, Thingstad F, Weinbauer MG, Bratbak G, Heldal M. (2008). Global-scale processes with a nanoscale drive: the role of marine viruses. *Isme Journal* **2**: 575–578.

Claquin P, Probert I, Lefebvre S. (2008). Effects of temperature on photosynthetic parameters and TEP production in eight species of marine microalgae. *Aquat Microb Ecol* **51**: 1–11.

Cochran P, Paul J. (1998). Seasonal abundance of lysogenic bacteria in a subtropical estuary. *Appl Environ Microbiol* **64**: 2308–2312.

Cottrell MT, Suttle CA. (1991). Wide-spread occurrence and clonal variation in viruses which cause lysis of a cosmopolitan, eukaryotic marine phytoplankter. *Mar Ecol Progr Ser* **78**: 1–9.

Cottrell MT, Suttle CA. (1995). Dynamics of lytic virus infecting the photosynthetic marine picoflagellate Micromonas pusilla. *Limnol Oceanogr* **40**: 730–739.

D'Amico S, Collins T, Marx J-C, Feller G, Gerday C. (2006). Psychrophilic microorganisms: challenges for life. *EMBO Rep* **7**: 385–389.

Dill K, Ghosh K, Schmit J. (2011). Physical limits of cells and proteomes. *Proc Natl Acad Sci USA* **108**: 17876–17882.

El-Sabaawi R, Harrison PJ. (2006). Interactive effects of irradiance and temperature on the photosynthetic physiology of the pennate diatom pseudo-nitzschia granii (bacillariophyceae) from the northeast subarctic pacific. *J Phycol* **42**: 778–785.

Evans C, Archer SD, Jacquet S, Wilson WH. (2003). Direct estimates of the contribution of viral lysis and microzooplankton grazing to the decline of a Micromonas spp. population. *Aquat Microb Ecol* **30**: 1–13.

Evans C, Pond DW, Wilson WH. (2009). Changes in Emiliania huxleyi fatty acid profiles during infection with E-huxleyi virus 86: physiological and ecological implications. *Aquat Microb Ecol* **55**: 219–228.

Foulon E, Not F, Jalabert F, Cariou T, Massana R, Simon N. (2008). Ecological niche partitioning in the picoplanktonic green alga Micromonas pusilla: evidence from environmental surveys using phylogenetic probes. *Environ Microbiol* **10**: 2433–2443.

Fuhrman JA. (1999). Marine viruses and their biogeochemical and ecological effects. *Nature* **399**: 541–548.

Guillou L, Eikrem W, Chrétiennot-Dinet M-J, Le Gall F, Massana R, Khadidja Romari, Pedros-Alio C, Vaulot D. (2004). Diversity of picoplanktonic prasinophytes Assessed by direct nuclear SSU rDNA sequencing of environmental samples and novel isolates retrieved from oceanic and coastal marine ecosystems. *Protist* **155**: 193–214.

Hingamp P, Grimsley N, Acinas SG, Clerissi C, Subirana L, Poulain J *et al.* (2013). Exploring nucleo-cytoplasmic large DNA viruses in Tara oceans microbial metagenomes. *ISME J* **7**: 1678–1695.

Jiang SC, Paul JH. (1996). Occurrence of lysogenic bacteria in marine microbial communities as determined by prophage induction. *Mar Ecol Progr Ser* **35**: 235–243.

Keller MD, Selvin RC, Claus W, Guillard RRL. (1987). Media for the culture of oceanic ultraphytoplankton. *J Phycol* **23**: 633–638.

Kendrick BJ, DiTullio GR, Cyronak TJ, Fulton JM, Van Mooy BAS, Bidle KD. (2014). Temperature-induced viral resistance in Emiliania huxleyi (Prymnesiophyceae). *PLoS One* **9**: e112134-14.

Knowles B, Silveira CB, Bailey BA, Barott K, Cantu VA, Cobián-Güemes AG *et al.* (2016). Lytic to temperate switching of viral communities. *Nature* **531**: 466–470.

Los DA, Murata N. (2004). Membrane fluidity and its roles in the perception of environmental signals. *Biochim Biophys Acta* **1666**: 142–157.

Mackinder LCM, Worthy CA, Biggi G, Hall M, Ryan KP, Varsani A *et al.* (2009). A unicellular algal virus, Emiliania huxleyi virus 86, exploits an animal-like infection strategy. *J Gen Virol* **90**: 2306–2316.

Marie D, Brussaard C, Thyrhaug R, Bratbak G, Vaulot D. (1999). Enumeration of marine viruses in culture and natural samples by flow cytometry. *Appl Environ Microbiol* **65**: 45–52.

Martínez-Martínez J, Boere A, Gilg I, Lent JWMV, Witte HJ, Bleijswijk JDLV *et al.* (2015). New lipid envelop-containing dsDNA virus isolates infecting Micromonas pusilla reveal a separate phylogenetic group. *Aquat Microb Ecol* **74**: 17–28.

Mayer JA, Taylor FJR. (1979). A virus which lyses the marine nanoflagellate Micromonas pusilla. *Nature* **281**: 299–301.

McDaniel L, Houchin LA, Williamson SJ, Paul JH. (2002). Lysogeny in marine Synechococcus. *Nature* **415**: 496–496.

McDaniel LD, delaRosa M, Paul JH. (2006). Temperate and lytic cyanophages from the Gulf of Mexico. *J Mar Biol Assoc UK* **86**: 517–527.

Mojica KDA, Brussaard CPD. (2014). Factors affecting virus dynamics and microbial host -virus interactions in marine environments. *FEMS Microbiol Ecol* **89**: 495–515.

Mojica KDA, Huisman J, Wilhelm SW, Brussaard CPD. (2015). Latitudinal variation in virus-induced mortality of phytoplankton across the North Atlantic Ocean. *ISME J* **10**: 500–513.

Monier A, Comte J, Babin M, Forest A, Matsuoka A, Lovejoy C. (2015). Oceanographic structure drives the assembly processes of microbial eukaryotic communities. *ISME J* **9**: 990–1002.

Nagasaki K, Yamaguchi M. (1998). Effect of temperature on the algicidal activity and the stability of HaV (Heterosigma akashiwo virus). *Aquat Microb Ecol* **15**: 211–216.

Not F, Latasa M, Marie D, Cariou T, Vaulot D, Simon N. (2004). A single species, Micromonas pusilla (Prasinophyceae), dominates the eukaryotic picoplankton in the western English Channel. *Appl Environ Microbiol* **70**: 4064–4072.

Peperzak L, Brussaard C. (2011). Flow cytometric applicability of fluorescent vitality probes on phytoplankton. *J Phycol* **47**: 692–702.

Ras M, Steyer J-P, Bernard O. (2013). Temperature effect on microalgae: a crucial factor for outdoor production. *Rev Environ Sci Biotechnol* **12**: 153–164.

Raven JA, Geider RJ. (1988). Temperature and algal growth. *N Phytol* **110**: 441–461.

Sahlsten E. (1998). Seasonal abundance in Skagerrak-Kattegat coastal waters and host specificity of viruses infecting the marine photosynthetic flagellate Micromonas pusilla. *Aquat Microb Ecol* **20**: 2207–2212.

Suttle CA. (2005). Viruses in the sea. *Nature* **437**: 356–361.

Suttle CA. (2007). Marine viruses—major players in the global ecosystem. *Nat Rev Microbiol* **5**: 801–812.

Taylor J. (1962). The estimation of numbers of bacteria by tenfold dilution series. *J Appl Bacteriol* **25**: 54–61.

Thomas R, Grimsley N, Escande M-L, Subirana L, Derelle E, Moreau H. (2011). Acquisition and maintenance of resistance to viruses in eukaryotic phytoplankton populations. *Environ Microbiol* **13**: 1412–1420.

Thomas R, Jacquet S, Grimsley N, Moreau H. (2012). Strategies and mechanisms of resistance to viruses in photosynthetic aquatic microorganisms. *Adv Oceanogr Limnol* **3**: 1–15.

Thomsen HA, Buck KR. (1998). Nanoflagellates of the central California waters: taxonomy, biogeography and abundance of primitive, green flagellates (Pedinophyceae, Prasinophyceae). *Deep Sea Res Pt II* **45**: 1–21.

Tomaru Y, Tanabe H, Yamanaka S. (2005). Effects of temperature and light on stability of microalgal viruses, HaV, HcV and HcRNAV. *Plankton Biol Ecol* **52**: 1–6.

Tomaru Y, Kimura K, Yamaguchi H. (2014). Temperature alters algicidal activity of DNA and RNA viruses infecting Chaetoceros tenuissimus. *Aquat Microb Ecol* **73**: 171–183.

Toseland A, Daines SJ, Clark JR, Kirkham A, Strauss J, Uhlig C *et al.* (2013). The impact of temperature on marine phytoplankton resource allocation and metabolism. *Nat Clim Change* **3**: 979–984.

Waters RE, Chan AT. (1982). Micromonas-Pusilla virus—the virus growth-cycle and associated physiological events within the host-cells—host range mutation. *J Gen Virol* **63**: 199–206.

Weinbauer MG, Suttle CA. (1999). Lysogeny and prophage induction in coastal and offshore bacterial communities. *Aquat Microb Ecol* **18**: 217–225.

Weinbauer MG, Christaki U, Nedoma J, Simek K. (2003). Comparing the effects of resource enrichment and grazing on viral production in a meso-eutrophic reservoir. *Aquat Microb Ecol* **31**: 137–144.

Wilhelm SW, Suttle CA. (1999). Viruses and nutrient cycles in the sea viruses play critical roles in the structure and function of aquatic food webs. *BioScience* **49**: 781–788.

Williamson SJ, Houchin LA, McDaniel L, Paul JH. (2002). Seasonal variation in lysogeny as depicted by prophage induction in Tampa Bay, Florida. *Appl Environ Microbiol* **68**: 4307–4314.

Wilson WH, Mann NH. (1997). Lysogenic and lytic viral production in marine microbial communities. *Aquat Microb Ecol* **13**: 95–100.

Wilson WH, Francis I, Ryan K, Davy SK. (2001). Temperature induction of viruses in symbiotic dinoflagellates. *Aquat Microb Ecol* **25**: 99–102.

Yau S, Grimsley N, Moreau H. (2015). Molecular ecology of Mamiellales and their viruses in the marine environment. *Perspect Phycol* **2**: 83–89.

Zingone A, Sarno D, Forlani G. (1999). Seasonal dynamics in the abundance of Micromonas pusilla (Prasinophyceae) and its viruses in the Gulf of Naples (Mediterranean Sea). *J Plankton Res* **21**: 2143–2159.

Zingone A, Natale F, Biffali E, Borra M, Forlani G, Sarno D. (2006). Diversity in morphology, infectivity, molecular characteristics and induced host resistance between two viruses infecting Micromonas pusilla. *Aquat Microb Ecol* **45**: 1–14.

Supplementary Information accompanies this paper on The ISME Journal website (http://www.nature.com/ismej)